Biochimica et Biophysica Acta 1840 (2014) 2222–2233

Contents lists available at ScienceDirect

Biochimica et Biophysica Acta

journal homepage: www.elsevier.com/locate/bbagen

G-quadruplex-mediated regulation of telomere binding protein POT1 gene expression

Qingqing He, Ping Zeng, Jia-Heng Tan, Tian-Miao Ou, Lian-Quan Gu, Zhi-Shu Huang, Ding Li *

School of Pharmaceutical Sciences, Sun Yat-sen University, Guangzhou University City, 132 Waihuan East Road, Guangzhou 510006, PR China

ARTICLE INFO

Article history:
Received 24 November 2013
Received in revised form 10 February 2014
Accepted 3 March 2014
Available online 12 March 2014

Keywords:
POT1
Shelterin
Telomere
G-quadruplex
hnRNP K
Cancer

ABSTRACT

Background: Telomere is protected by its G-quadruplex, T-loop structure, telomerase, and binding protein complex. Protein POT1 (protection of telomeres 1) is one subunit of telomere binding protein complex Shelterin. POT1 acts as a regulator of telomerase-dependent telomere length, and it can help telomere to form D-loop structure to stabilize telomere. POT1 protects telomere ends from ATR-dependent DNA damage response as well.
Methods: Extensive methods were used, including CD, EMSA, ITC, PCR stop assay, luciferase reporter assay, quantitative real-time PCR, Western blot, chromatin immunoprecipitation (Ch-IP), cloning, expression and purification of proteins.
Results: We found a new G-rich 30-base-pair long sequence (P-pot1 G18) located from −165 to −136 base pairs upstream of the translation starting site of protein POT1. This sequence in the promoter region of pot1 gene formed G-quadruplex resulting in down-regulation of pot1 gene transcription. This G-rich sequence is close to a binding site "TCCC" for transcription factor hnRNP K (heterogeneous nuclear ribonucleoprotein K), and its conversion to G-quadruplex prevented the access of hnRNP K to this binding site. The binding of hnRNP K could up-regulate pot1 gene transcription. TMPyP4 (meso-tetra(*N*-methyl-4-pyridyl)porphine) has been widely used as G-quadruplex binding ligand, which stabilized the G-quadruplex in vitro and in cellulo, resulting in down-regulation of pot1 gene transcription.
Conclusions: This G-quadruplex might become a potentially new drug target for antitumor agents.
General significance: Our results first demonstrated that G-quadruplex formation can affect the binding of transcription factor to its nearby binding site, and thus making additional influence to gene transcription.

1. Introduction

Telomeres are protein–DNA structures, which are present at the ends of all eukaryotic linear chromosomes [1,2]. Loss of telomeres would lead to unwanted end to end chromosomal fusions, nucleolytic degradation, recombination with chromosome-internal DNA, cell proliferative arrest, senescence and apoptosis [3,4]. In human, telomere DNA consists of a simple tandem array of the sequence (TTAGGG)n which is highly conserved throughout evolution [5]. Telomere length is mediated by its DNA structure, its associated proteins, and telomerase acting as a reverse transcriptase to produce telomeric repeats with a template [6]. The double-stranded telomeric DNA ends in a 3′ single stranded overhang of 150 to 300 base pairs (bp) which is believed to be required for a higher order structure such as T-loop structure or G-quadruplex [7]. Telomeres are protected by a multi-protein complex called Shelterin, which has six subunits including the double-stranded telomeric repeat binding factors TRF1 and TRF2, and their interacting proteins RAP1 (repressor activator protein 1) and TIN2 (TRF1-interacting nuclear protein 2), and the G-strand overhang binding protein POT1 (protection of telomeres 1) and its binding partner protein TPP1 (formerly known as TINT1, PTOP, or PIP1) [8]. TIN2 is the central component of Shelterin, which tethers TRF1 and TRF2 to POT1/TPP1 [9]. TRF1 is a negative regulation factor of telomere length [10]. TRF2 is a second negative regulator of telomere length, since overexpression of TRF2 can lead to progressive shortening of telomere length [11]. TPP1 is also known as the missing β-subunit of POT1, which can increase affinity of POT1 with telomeric single stranded DNA and then increase process activity of telomerase [12].

Human POT1 is located on chromosome 7 with NCBI reference sequence number of NG_029232, and is linked to Shelterin complex by TPP1 protein through its *C*-terminus. POT1 has two OB folds (oligonucleotide/oligosaccharide binding) in its *N*-terminus, and binds to the 3′-single strand TTAGGG tandem repeat sequence by its OB folds. The first OB fold of POT1 combines with 5′-TTAGGG while the second fold associates with downstream TTAG-3′ [13]. The binding direction of POT1 is from 3′ to 5′ of DNA overhang substrate. POT1–TPP1 complex can move forth and back on the telomeric overhang, in order to promote telomere G-quadruplex folding and unfolding to have an influence on telomerase [14]. POT1 acts as a regulator of telomerase-dependent telomere length, and it can help telomere to form D-loop

* Corresponding author. Fax: +86 20 3994 3058.
E-mail address: liding@mail.sysu.edu.cn (D. Li).

http://dx.doi.org/10.1016/j.bbagen.2014.03.001
0304-4165/

structure to stabilize telomere. POT1 protects telomere ends from ATR-dependent DNA damage response as well [15]. Mutation of POT1 causes dysfunction of telomere such as SCFs (sister chromatid-type end-to-end fusions), chromosomal breaks, and fusion in chronic lymphocytic leukemia [16].

G-quadruplex formed by guanine-rich DNA sequence is a kind of non-B-form DNA structure that exists in human genome, especially in sub-telomere, gene bodies and gene regulatory regions [17]. It has been shown that G-quadruplex structure indeed exists in genomic DNA isolated from human cancer cells by using structure-specific antibody [18]. G-quadruplex plays a key role in biological processes such as transcriptional regulation, DNA replication, and genome stability, which makes G-quadruplex to be a potentially important therapeutic target [19]. More and more G-quadruplexes have been found in gene promoter region, which can affect the expression of essential genes, including *c-myc*, *c-kit*, *bcl-2*, *kras* and VEGF. It has been shown that G-quadruplex formed in nuclease hypersensitivity element III1, upstream of *c-myc* P1 promoter has biological relevance with c-MYC protein expression [20].

In the present study, we found a 30-base-pair G-rich sequence located from −165 to −136 base pairs upstream of the translation starting site of POT1 by using the UCSC Genome Browser Home website. This sequence in the promoter region of the pot1 gene could form G-quadruplex, resulting in down-regulation of pot1 gene transcription. This G-rich sequence is close to a binding site "TCCC" for transcription factor hnRNP K (heterogeneous nuclear ribonucleoprotein K), and its formation of G-quadruplex prevented the access of hnRNP K to this binding site. The binding of hnRNP K could up-regulate pot1 gene transcription. TMPyP4 (meso-tetra(*N*-methyl-4-pyridyl)porphine) has been widely used as a G-quadruplex binding ligand [21], which could stabilize the G-quadruplex in vitro and in cellulo, resulting in down-regulation of pot1 gene transcription. Our experimental studies showed that this G-quadruplex might become a potentially new drug target for antitumor agents. Our present results first demonstrated that G-quadruplex formation can affect the binding of transcription factor to its nearby binding site, and thus making additional influence to gene transcription.

2. Materials and methods

2.1. DNA sample

DNA oligonucleotides were purchased from Invitrogen and HPLC purified, which were stored at −20 °C. DNA concentration was measured by using nanodrop ND-1000 ultramicro UV–Vis spectrophotometer (Thermo Fisher Scientific Inc., Waltham, MA).

2.2. Circular dichroism

Circular dichroism (CD) spectra were normally recorded at 25 °C on a JASCO-815 spectropolarimeter by using a 1 cm path length quartz cuvette with a reaction volume of 700 μL. The DNA oligonucleotides were typically prepared in 5 μM solution in 10 mM Tris–HCl, pH 7.5, containing 100 mM KCl or 100 mM NaCl. The DNA samples were heat-denatured at 95 °C for 5 min, and then gradually cooled to room temperature for various studies. Each sample was scanned twice, and the average was taken as the depicted data. The DNA sample was scanned from 220 nm to 320 nm with 2 s collection time per data point, and then the sample buffer was subtracted. For CD melting experiment, except for setting the detection temperature from 20 °C to 90 °C, all other parameters remained unchanged.

2.3. Gel electrophoresis

The structure formed by DNA oligonucleotides can be detected by nondenaturing polyacrylamide gel electrophoresis (PAGE) because their difference in gel migration properties, which can be caused by molecular size, shape and charge of DNA oligonucleotides. The 10 μM DNA samples were prepared in a 10 mM Tris–HCl (pH 7.5) buffer supplemented with 100 mM KCl or 100 mM NaCl. The DNA samples were heat-denatured at 95 °C for 5 min and subsequently cooled to room temperature. The DNA samples were loaded on a 16% polyacrylamide gel and run at 120 V, with 10% sucrose added just before loading. After staining with 1× Gel-Red, the gels were imaged by using UV-shadowing.

2.4. Isothermal titration calorimetry (ITC)

ITC experiment was carried out in a VP-ITC titration calorimeter (MicroCal, Northampton, MA). All samples were thoroughly degassed, and the reference cell was filled with the degassed buffer before loading. P-pot1 G18 G-quadruplex DNA (5 μM) was transferred into a sample cell of 2 mL, and TMPyP4 (300 μM) in the same buffer was kept in syringe with volume of 300 μL. A total of 30 injections were carried out, with 300 s spacing time, 10 μL injection volume, and 20 μL duration for each titration at 25 °C. The blank control sample was measured in parallel experiments by injecting TMPyP4 solution of the same concentration to solution buffer. The blank control sample was subtracted from the corresponding binding experiments prior to curve fitting. The thermograms obtained in ITC experiments were fit with proper model in Origin 8.0.

2.5. PCR stop assay

Sequences of the tested DNA oligonucleotides (P-pot1 G18 or Mut P-pot1 G18) and the corresponding complementary sequence (P-pot1 G18 rev) used are listed in Table 1. The reaction was performed in 1× PCR buffer, containing 2 μM of each pair of oligonucleotides, 0.16 mM dNTP, 2.5 U *Taq* polymerase, and compound at a certain concentration. Reaction mixtures were incubated in a thermocycler with the following cycling conditions: a denaturing cycle of 94 °C for 3 min, followed by 10 cycles of 94 °C for 30 s, 59 °C for 30 s and 72 °C for 30 s. Amplified products were resolved on 16% nondenaturing polyacrylamide gels in

Table 1
Oligonucleotide sequences used in the present study.

Name	Sequence (5′–>3′)
P-pot1 G18	AGGGGAAGCGGGCGGGTCCGCTGGGCGGGA
Mut P-pot1 G18	AGGGGAAGCAAACAAATCCGCTAAACGGGA
P-pot1 G18 rev	GCTTCCCCTAAGCTTGCCTCCCGCC
P-pot1 G18 Mut1	AAAAGAAGCGGGCGGGTCCGCTGGGCGGGA
P-pot1 G18 Mut2	AGAAAAAGCGGGCGGGTCCGCTGGGCGGGA
P-pot1 G18 Mut3	AGGGGAAGCAAACGGGTCCGCTGGGCGGGA
P-pot1 G18 Mut4	AGGGGAAGCGGGCGGGTCCGCTAAACGGGA
P-pot1 G18 Mut5	AGGGGAAGCGGGCGGGTCCGCTGGGCAAAA
P-pot1 G18 tccc	AGGGGAAGCGGGCGGGTCCGCTGGGCGGGATTTGAGCTTCCCTTT
POT1 S	CGACGCGCTAGCTCTTTGGTTCCAGCAACAAATTATATAT
POT1 A	CTGCAGCTCGAGTTAGATTACATCTTCTGCAACTGTGG
β-Actin S	GCATCCTGTCGGCAATGC
β-Actin A	GTTGCTATCCAGGCTGTGC
qβ-Actin A	GTTGCTATCCAGGCTGTGC
qβ-Actin S	CCAGACGCAGGATGGCATG
qPOT1 A	TCACCAGCTCTGGCTTTGC
qPOT1 S	GATGCCCAAACACGTAAGGC
hnRNP K A	CTAGCTAGCGAAACTGAACAGCCAGAAGAAA
hnRNP K S	CCGCTCGAGTTAGAAAAACTTTCCAGAATACTG
Ch-IPP-pot1 A	GTAAAGACTGCAGTAGGTGCC
Ch-IP P-pot1 S	GGAATTGTCGCAGCTCCCCT
pEGFP–hnRNP K A	CTAGCTAGCATGGAAACTGAACAGCCAGAAG
pEGFP–hnRNP K S	CCGCTCGAGGAAAAACTTTCCAGAATACTGCTTt
siRNA-hnRNP K A	AAUUCCUCCUGCUAGACUCtt
siRNA-hnRNP K S	GAGUCUAGCAGGAGGAAUUtt

0.5× TBE and 1× Gel-Red stained. IC_{50} values were calculated using optical density read from image J software.

2.6. Cell culture and treatment with TMPyP4

Hela cell culture was maintained on DMEM medium supplemented with 10% fetal bovine serum, 100 U/mL penicillin and 100 μg/mL streptomycin in 25 cm^2 culture flasks at 37 °C humidified atmosphere with 5% CO_2. For the compound treatment experiment, Hela cells were harvested from the culture during exponential growth phase, seeded into multi-well culture plates at 5×10^4 cells/mL in fresh medium, and then treated with TMPyP4 at certain concentrations for 48 h.

2.7. Plasmid construction

DNA fragment from −1000 bp to −1 bp of human pot1 gene promoter region, containing wild type P-pot1 G18 sequence (from −165 to −136), was amplified from A549 cell total DNA by using PCR. This fragment was then inserted into pMetLuc-Reporter vector (Clontech) to give a recombinant plasmid, named as P-pot1 G18 construct. As for Mut P-pot1 G18, site-directed mutations were made to P-pot1 G18 region of the construct as shown in Fig. 5.

2.8. Transfection and luciferase assays

After each well of 2×10^6 Hela cells were taken board, 0.18 μg P-pot1 G18 plasmid DNA or Mut P-pot1 G18 plasmid DNA and 0.02 μg pRL-TK (Promega) were co-transfected into Hela cells using Amaxa Cell Line Nucleofector Kit V (Lonza). Then transfected medium was removed and different concentrations of TMPyP4 were added into the medium after 6 h of transfection. After another 48 h of drug treatment, luciferase activity was evaluated by using Ready-To-Glow Secreted Luciferase Reporter System (Clontech) and Renilla Luciferase Assay System (Promega).

2.9. Real-time PCR

Total RNA was used as a template for reverse transcription using the following protocol: each 20 μL reaction contained 1× M-MLV buffer, 125 μM dNTP, 100 pmol oligo dT18 primer, 100 units of M-MLV reverse transcriptase, DEPC treated water, and 2 μg of total RNA. Briefly, RNA and oligomer dT18 primer were incubated at 70 °C for 10 min, and then immediately placed on ice, after which the other components were added and incubated at 42 °C for 1 h, and then at 70 °C for 15 min. Finally, the reacted solution was stored at −20 °C. The total volume of 20 μL of real-time RT-PCR reaction mixtures contained 2 μL 10× PCR buffer, 500 μmol/L dNTPs, 0.15 μM each primer shown in Table 1 (POT1 S/POT A; *β-actin* S/*β-actin* A), 1 μL cDNA template, 1 U Dream *Taq* DNA polymerase, and nuclease-free water. The protocol used for real-time RT-PCR includes a denaturing cycle of 5 min at 95 °C, 30 cycles of PCR (94 °C for 1 min, 58 °C for 50 s, 72 °C for 2.5 min), and then holding at 10 °C. The PCR products were mixed with loading buffer, and then loaded in 1.2% agarose gel. After electrophoresis, the gel was imaged by using UV-shadowing.

2.10. Quantitative real-time RT-PCR

cDNA samples of Hela cells were from the real-time RT-PCR. The total volume of 25 μL of quantitative reaction mixtures contained 12.5 μL of SYBR Premix ExTaq (Takara), 0.4 μM each of forward and reverse primers as shown in Table 1 (qβ-actin A, qβ-actin S, qPOT1 A, qPOT1 S), 1 μL cDNA, and nuclease-free water. The program used for all genes consisted of a denaturing cycle of 7 min at 95 °C, 45 cycles of PCR (95 °C for 10 s, 60 °C for 30 s), a melting cycle consisting of 95 °C for 15 s, 60 °C for 15 s, and a step cycle starting at 60 °C with a 0.2 °C/s transition rate to 95 °C. The specificity of real-time RT-PCR product was confirmed by melting curve analysis. Three replications were performed, and then pot1 gene mRNA level was normalized to β-actin mRNA level of each sample. Results of real-time PCR were analyzed using the $2^{-\Delta CT}$ method to compare the transcriptional levels of pot1 gene in each sample relative to non-compound-treated control.

2.11. Western blot

After Hela cells were taken board for each well of 2×10^6 and then treated with different concentrations of TMPyP4 for 48 h, the cells harvested from each well of culture plates were lysed in 50 μL of protein extraction buffer consisting of 1 mM PMSF for 30 min. The suspension was centrifuged at 10,000 rpm at 4 °C for 5 min, and the protein content of supernatant was measured by using BCA assay. The same amount of protein for each sample was loaded onto 12% polyacrylamide gel, and then transferred to a microporous polyvinylidene difluoride (PVDF) membrane. Western blotting was performed by using anti-POT1 (ab21382, abcam), anti-hnRNP K (ab39975, abcam) and anti-β-actin (cell signaling technology) antibodies, as well as horseradish peroxidase-conjugated anti-rabbit secondary antibody and anti-mouse secondary antibody. Protein bands were visualized by using chemiluminescence substrate.

2.12. pET-28a–hnRNP K plasmid construction and hnRNP K protein expression and purification

The vector used in the plasmid construct was pET-28a(+), which was restriction digested with NheI and XhoI. The full length hnRNP K protein DNA sequence was cloned by using the following two primers: hnRNP K A (5′-CTAGCTAGCGAAACTGAACAGCCAGAAG AAA-3′) and hnRNP K S (5′-CCGCTCGAGTTAGAAAAACTTTCCAGAA TACTG-3′). The PCR protocol was as follows: a denaturing cycle of 5 min at 94 °C, 30 cycles of PCR (94 °C for 1 min, 56 °C for 1 min 15 s, 72 °C for 2.5 min). The pET-28a–hnRNP K recombinant plasmid was transformed into DH5α, spread on medium containing 0.1 mg/mL Kanamycin, and then single colony was picked to enlarge cultivation. After confirmation by sequencing, the recombinant pET-28a–hnRNP K plasmid was transformed into BL21::DE3, and then the cells were grown to an optical density of 0.5 at 595 nm. Isopropyl-β-D-thiogalactopyranoside was added to a concentration of 0.2 mM, and bacteria were induced for 5 h. The recombinant protein was then purified with HiTrap column following manufacture's protocol. The pure protein was used for EMSA and CD experiments.

2.13. Chromatin immunoprecipitation

Ch-IP experiment was performed with EZ-Magna Ch-IP™ A one-day Chromatin Immunoprecipitation kit (Millipore) following manufacturer's protocol. After 2 days of collection of about 1×10^7 Hela cells in a 25 cm^2 culture dish, the cells were fixed with 1% formaldehyde for 15 min and then lysed. The cells were sonicated to shear the chromatin to a manageable size of 200−1000 bp of DNA fragments by using a SCIENTZ-II D sonicator (SCIENTZ). Ch-IP class hnRNP K mouse monoclonal antibody (ab39975, abcam) was used to immunoprecipitate chromatin in Hela cells. Anti-rabbit IgG was used for mock immunoprecipitation. Ch-IP was kept swinging overnight at 4 °C, and immune complexes were collected by using protein A magnetic beads provided in the kit. Immunoprecipitated DNA was obtained after protein was put away from immunoprecipitated chromatin with proteinase K. Immunoprecipitated DNA samples were amplified by using PCR to show hnRNP K occupancy of POT1 protein promoter and negative control in cellulo. The PCR protocol was as follows: a denaturing cycle of 3 min at 94 °C, 32 cycles of PCR (94 °C for 20 s, 60 °C for

30 s, and 72 °C for 30 s). The primers (Ch-IP P-pot1 A/Ch-IP P-pot1 S) used for PCR were shown in Table 1.

2.14. Co-transfection and luciferase assays

The vector used in the plasmid construction was pEGFP-N3, and the hnRNP K gene was obtained from pET-28a–hnRNP K plasmid by using PCR. After each well of 2×10^6 Hela cells were taken board, pEGFP-N3 and pEGFP–hnRNP K or NC and siRNA hnRNP K primers were transfected into Hela cells, respectively. After 4 h of incubation, the medium was removed, and 0.18 μg P-pot1 G18 plasmid DNA and 0.02 μg pRL-TK (Promega) were co-transfected into the Hela cells. After 36 h of over-expression or RNA interference, luciferase activity was measured by using Ready-To-Glow Secreted Luciferase Reporter System (Clontech) and Renilla Luciferase Assay System (Promega).

2.15. Transfection and Western blot

After each well of 2×10^6 Hela cells were taken board, pEGFP-N3 and pEGFP–hnRNP K or NC and siRNA hnRNP K primers were transfected into Hela cells, respectively. Transfection medium was replaced by the fresh medium after 6 h of transfection. After the 36 h over-expression or RNA interference, the cells were harvested, and the POT1 protein translation levels were measured through Western blot, as introduced in Section 2.11.

3. Results

3.1. P-pot1 G18 oligonucleotide formed G-quadruplex in vitro

Guanine-rich sequences have a tendency to fold into G-quadruplex, and parallel and anti-parallel G-quadruplexes display different characteristic CD spectra. The parallel G-quadruplex normally shows a positive band at 260 nm and a negative band around 240 nm, while anti-parallel G-quadruplex usually generates a large positive band at 290 nm, a small positive band at 245 nm, and a negative band at 260 nm [22]. In the present study, we found a 30-base-pair G-rich sequence (named as P-pot1 G18) located from −165 to −136 base pairs upstream of the translation starting site of POT1 through the UCSC Genome Browser Home website (Fig. 1). In order to know whether P-pot1 G18 could fold into G-quadruplex, CD experiment was carried out, and its spectrum has a characteristic positive peak around 260 nm, a valley at 240 nm, and a small peak at 285 nm in buffer solution containing NaCl (Fig. 2A), indicating a mixed type G-quadruplex. Its absorption at 260 nm was not changed with increasing concentration of NaCl. In comparison, its absorption spectrum is quite different in a solution containing KCl (Fig. 2B). P-pot1 G18 displays a peak at 260 nm and a valley at 240 nm, which is a typical characteristic of parallel G-quadruplex. The absorption of 260 nm increases obviously with increasing concentration of KCl. These results showed that P-pot1 G18 folded into G-quadruplex in vitro, while the types of G-quadruplexes formed in different monovalent-containing buffers are different.

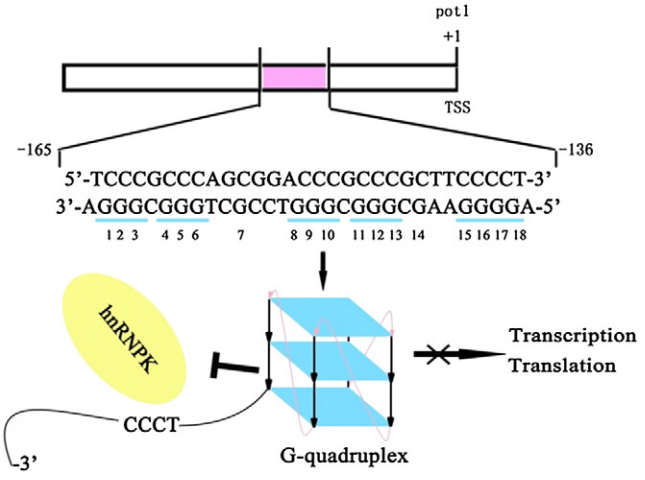

Fig. 1. G-rich strand in the pot1 promoter and its possible biological function upon its conversion into G-quadruplex.

Then, the secondary structure of P-pot1 G18 was studied with EMSA (electrophoretic mobility shift assay) to better understand its property. P-pot1 G18 with a length of 30 bp was found to fold into a secondary structure with a length of less than 20 bp in the presence of monovalent cation after heating to 95 °C followed with natural annealing to room temperature. This indicated that the folded G-quadruplex is likely to be an intra-molecular G-quadruplex. Our EMSA result in NaCl-containing buffer is a little different from that in KCl-containing buffer, and more higher order structures may exist in KCl-containing buffer rather than NaCl-containing buffer (Fig. 2C).

P-pot1 G18 has five guanine-rich sections, therefore, it may have some varying types of G-quadruplex topologies. We further studied these guanine-rich sections through mutagenesis, with our mutation sequences (Mut1–5) shown in Table 1. Based on their CD spectra, all mutated oligonucleotides were folded into parallel G-quadruplex structures in KCl-containing buffer as shown in Fig. 3A, which are similar to that of the wild-type P-pot1 G18. However, our further EMSA experimental results indicated that their secondary structures have some difference based on the retention time, as shown in Fig. 3B. The secondary structures of Mut4 and Mut5 look similar to that of the wild-type P-pot1 G18, while those of Mut1, Mut2, and Mut3 look quite different. In comparison, all oligonucleotides look somehow different in NaCl-containing buffer, based on their CD spectra. They all produced a positive peak at 260 nm and a negative peak around 240 nm, but with some differences at other wavelengths and peak intensities (Fig. 3C). Our further EMSA experimental results indicated that their secondary structures have some difference in NaCl-containing buffer based on the retention time as shown in Fig. 3D. The secondary structures of Mut4 and Mut5 look similar to that of the wild-type P-pot1 G18, while those of Mut1, Mut2, and Mut3 seem quite different. Our above results show that all wild-type and mutated P-pot1 G18 oligonucleotides can fold into G-quadruplex, while their G-quadruplex secondary structures can be different depending on mutating position and monovalent cation in the buffer.

3.2. TMPyP4 enhanced thermostability of the P-pot1 G18 G-quadruplex

TMPyP4 is a widely used G-quadruplex binding ligand, which can stabilize the G-quadruplex structure in the P1 promoter of c-*myc* resulting in suppression of c-*myc* transcription [23]. In the present study, we investigated whether TMPyP4 could also stabilize P-pot1 G18 G-quadruplex by using CD melting experiment through analyzing its CD absorption change at 260 nm in the presence or absence of TMPyP4 at temperature range from 20 °C to 90 °C in buffer containing NaCl or KCl. We obtained its CD spectra reading at 260 nm at varying temperatures, and then making curve fitting of these data to obtain *Tm* values (Supporting Information Figure S1). The *Tm* value of P-pot1 G18 in NaCl-containing buffer was determined to be 46.5 ± 0.7 °C (Table 2), while the addition of TMPyP4 increased its *Tm* value to 51.1 ± 1.1 °C. TMPyP4 could also increase the thermostability of P-pot1 G18 in KCl-containing buffer. The *Tm* value of P-pot1 G18 was determined to be 70.6 ± 0.5 °C in KCl-containing buffer, while the addition of TMPyP4 increased its *Tm* value to 83.9 ± 2.9 °C. Our results indicated that P-pot1 G18 was more stable in KCl-

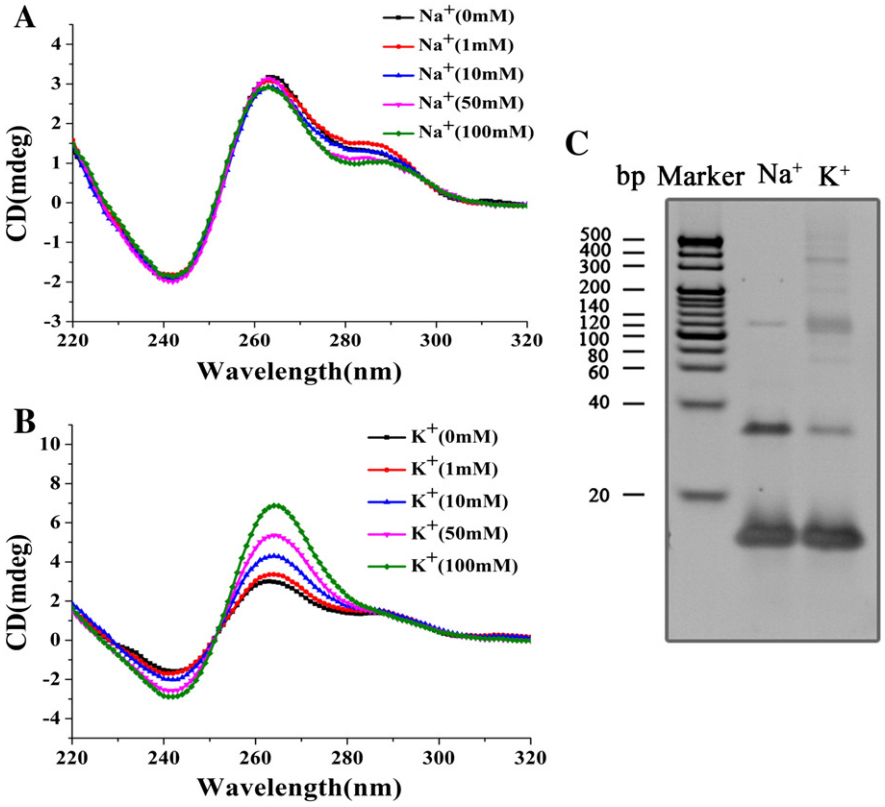

Fig. 2. G-quadruplex formed by P-pot1 G18 sequence in vitro. A. Circular dichroism spectrum for P-pot1 G18 in 10 mM Tris–HCl (pH 7.5) buffer containing varying concentrations of NaCl at 0, 1, 10, 50, and 100 mM. B. Circular dichroism spectrum for P-pot1 G18 in 10 mM Tris–HCl (pH 7.5) buffer containing varying concentrations of KCl at 0, 1, 10, 50 and 100 mM. C. EMSA for P-pot1 G18 oligonucleotide, in buffer containing NaCl or KCl.

containing buffer rather than NaCl-containing buffer, which is consistent with a previous report for other G-quadruplexes [24]. Our results also indicated that TMPyP4 enhanced the thermostability of P-pot1 G18 G-quadruplex significantly in KCl-containing buffer, however much less significantly in NaCl-containing buffer, which may be related with binding mode of TMPyP4 with the G-quadruplex influenced by different monovalent cations. It has been reported that TMPyP4 has different binding modes to G-quadruplex in the presence of different monovalent cations [25], and the nature of metal ion within the complex has an influence on the stacking interaction of TMPyP4 with G-quadruplex [26].

3.3. Thermodynamic study for the binding of TMPyP4 to the P-pot1 G18 G-quadruplex

In order to gain further understanding for the binding interactions between TMPyP4 and P-pot1 G18 G-quadruplex, we carried out ITC experiment to study their binding affinity. ITC is a valuable method to learn the binding affinity between molecules [27]. Here we titrated the P-pot1 G18 G-quadruplex with TMPyP4 in buffer containing NaCl or KCl, and the thermograms of these experiments are shown in Fig. 4. The reactions under both conditions exhibited just one binding process, and the thermodynamic parameters were determined as shown in Table 3. The primary binding constant K values were determined to be 4.62×10^5 in buffer containing 100 mM NaCl, and 1.91×10^5 in buffer containing 100 mM KCl, indicating that TMPyP4 binds tightly with P-pot1 G18 G-quadruplex under both experimental conditions. The binding stoichiometry between P-pot1 G18 G-quadruplex and TMPyP4 was determined to be 1:1 under both experimental conditions. The binding processes are both exothermic and enthalpy driven, because of small positive $T\triangle S$ values compared with large negative $\triangle H$ values. This result also supported that TMPyP4 bound tightly with P-pot1 G18 G-quadruplex.

3.4. The P-pot1 G18 G-quadruplex formation down-regulated pot1 gene transcription studied through luciferase assay with recombinant reporter plasmid

In order to know the role of P-pot1 G18 in the transcription of pot1 gene, we constructed a recombinant reporter plasmid with pot1 promoter region from −1000 bp to −1 bp inserted into the MCS region of Met-Luc Reporter plasmid (Fig. 5), and consequently expression of luciferase can be regulated by this pot1 promoter. Then, we had P-pot1 G18 sequence from −165 bp to −136 bp of pot1 promoter removed from this plasmid to give a deletion plasmid named as Del P-pot1 G18. We compared luciferase expression levels of these two plasmids, and Del P-pot1 G18 was found to have 59.1% ±14.6% reduced luciferase activity compared with the wild-type, as shown in Fig. 6A. This result indicated that P-pot1 G18 sequence should play an important role in the regulation of pot1 gene transcription. Many transcription factors play important roles in gene expression. It is possible that the removal of this G-rich sequence prevents the binding of transcription factors such as SP1 and NM23-H2, resulting in down-regulation of pot1 transcription.

Since P-pot1 G18 could form G-quadruplex in vitro, in order to know whether the formation of the G-quadruplex could affect pot1 gene transcription, we mutated P-pot1 G18 to disrupt its G-quadruplex formation and then studied the effect of this mutation on pot1 gene transcription. We made several G to A mutations in the middle region of P-pot1 G18 sequence, which was named as Mut P-pot1 G18 (Table 1). The CD spectrum of Mut P-pot1 G18 displays a positive peak around 275 nm and a negative peak around 250 nm (Fig. 6B), and the CD spectra of Mut P-pot1 G18 in buffer

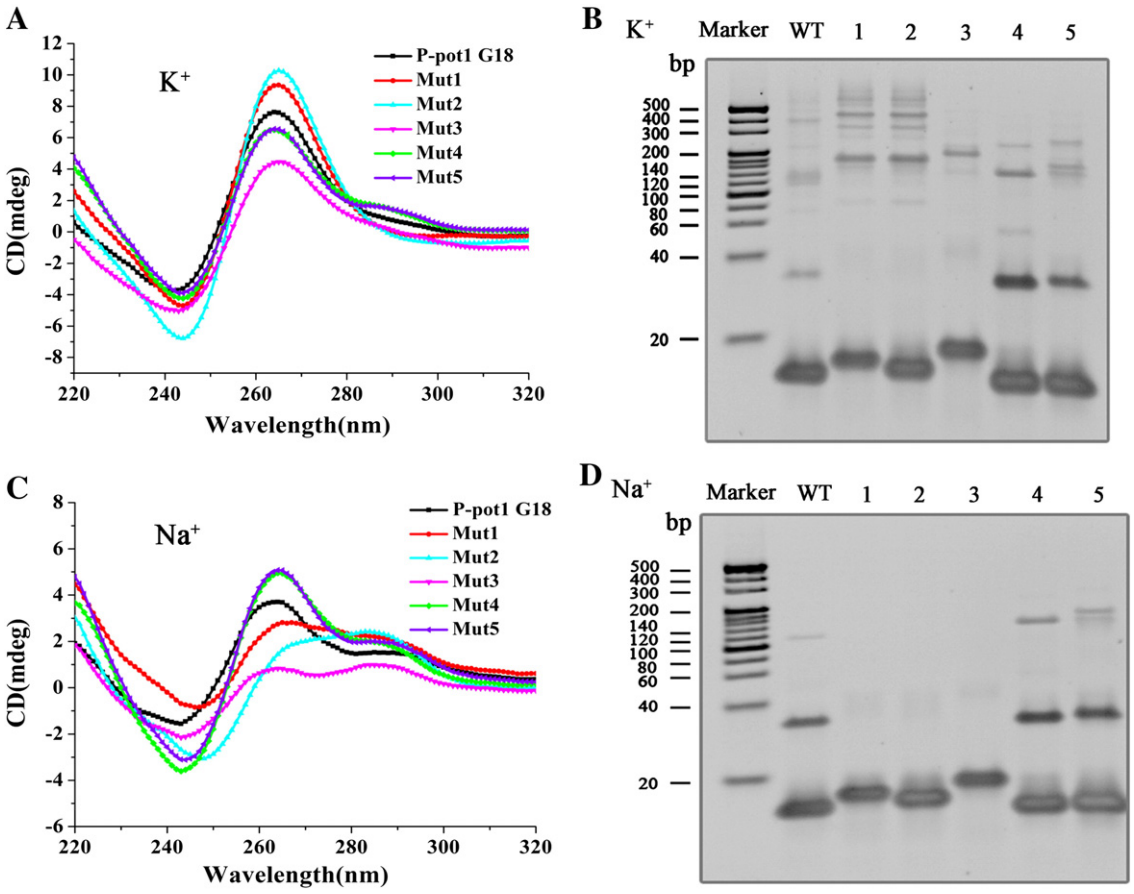

Fig. 3. P-pot1 G18 mutants could fold into G-quadruplex in vitro. A. Circular dichroism spectra for P-pot1 G18 and Mut1 to Mut5 oligonucleotides in 10 mM Tris–HCl buffer (pH 7.5), containing 100 mM KCl. The final DNA sample concentration was 5 μM. B. EMSA for P-pot1 G18 and Mut1 to Mut5 oligonucleotides in buffer containing KCl, and the final DNA sample concentration was 10 μM. Lane WT is for P-pot1 G18, and lanes 1 to 5 are for Mut1, Mut2, Mut3, Mut4, and Mut5, respectively. C. Circular dichroism spectra for P-pot1 G18 and Mut1 to Mut5 oligonucleotides in 10 mM Tris–HCl buffer (pH 7.5), containing 100 mM NaCl. D. EMSA for P-pot1 G18 and Mut1 to Mut5 oligonucleotides in buffer containing NaCl. Except monovalent cation difference in the buffer, other experimental conditions are the same as those of B.

containing NaCl or KCl are the same. This CD result indicated that Mut P-pot1 G18 could not form G-quadruplex in buffer with different monovalent cations in vitro. EMSA result also showed that the secondary structure of Mut P-pot1 G18 is significantly different from that of the wild type (Fig. 6C). Therefore, Mut P-pot1 G18 could not fold into G-quadruplex in vitro.

Then, we analyzed and compared the effect of TMPyP4 on P-pot1 G18 and Mut P-pot1 G18 in vitro. PCR stop assay can be used to analyze molecular extension on a template, which normally stops if the template folds into a stable secondary structure. Here, TMPyP4 was incubated with the wild type or mutant template, which was then subjected to PCR stop assay analysis (Fig. 6D). The IC_{50} value for the effect of TMPyP4 on P-pot1 G18 was determined to be 1.24 ± 0.27 μM by using Origin8.0, while the IC_{50} value for its effect on Mut P-pot1 G18 was determined to be 3.94 ± 0.21 μM. This result showed that the stabilization effect of TMPyP4 on P-pot1 G18 was higher than that on Mut P-pot1 G18 in vitro.

Table 2
Tm values for circular dichroism variable temperature experiment in NaCl and KCl-containing buffer.

	P-pot1 G18 (5 μM) (°C)	P-pot1 G18 : TMPyP4 (5 μM : 5 μM) (°C)
100 mM NaCl	46.5 ± 0.7	51.1 ± 1.1
100 mM KCl	70.6 ± 0.5	83.9 ± 2.9

Next, we studied the effect of the secondary structure formed by P-pot1 G18 or Mut P-pot1 G18 on pot1 gene transcription through luciferase assay with recombinant reporter plasmids. As shown in Fig. 6E, after treatment with increasing concentration of TMPyP4 for 48 h, the luciferase activity of the wild-type plasmid with P-pot1 G18 decreased significantly in a dose-dependent manner. In comparison, for variant plasmid with Mut P-pot1 G18, its luciferase activity decreased only slightly after incubation with increasing concentration of TMPyP4. This result showed that the G-quadruplex formed by P-pot1 G18 could down-regulate the pot1 gene transcription.

3.5. The P-pot1 G18 G-quadruplex formation down-regulated pot1 gene transcription in cancer cells

After above luciferase assay experiments with recombinant reporter plasmids, we would like to know whether the G-quadruplex formed by P-pot1 G18 could down-regulate pot1 gene transcription in cancer cells. Here, we used both normal RT-PCR and quantitative RT-PCR to study the mRNA expression level of gene. RT-PCR is a semi-quantitative method, while quantitative RT-PCR can monitor real-time PCR process. After Hela cells were incubated with an increasing concentration of TMPyP4 for 48 h, decreasing pot1 mRNA levels were detected through RT-PCR experiment, as shown in Fig. 7A. Then, quantitative RT-PCR was carried out to accurately study and compare the mRNA levels for the sample treated with 6.25 μM TMPyP4 and control, and it was found that 6.25 μM TMPyP4 could down-regulate about 50% pot1 mRNA

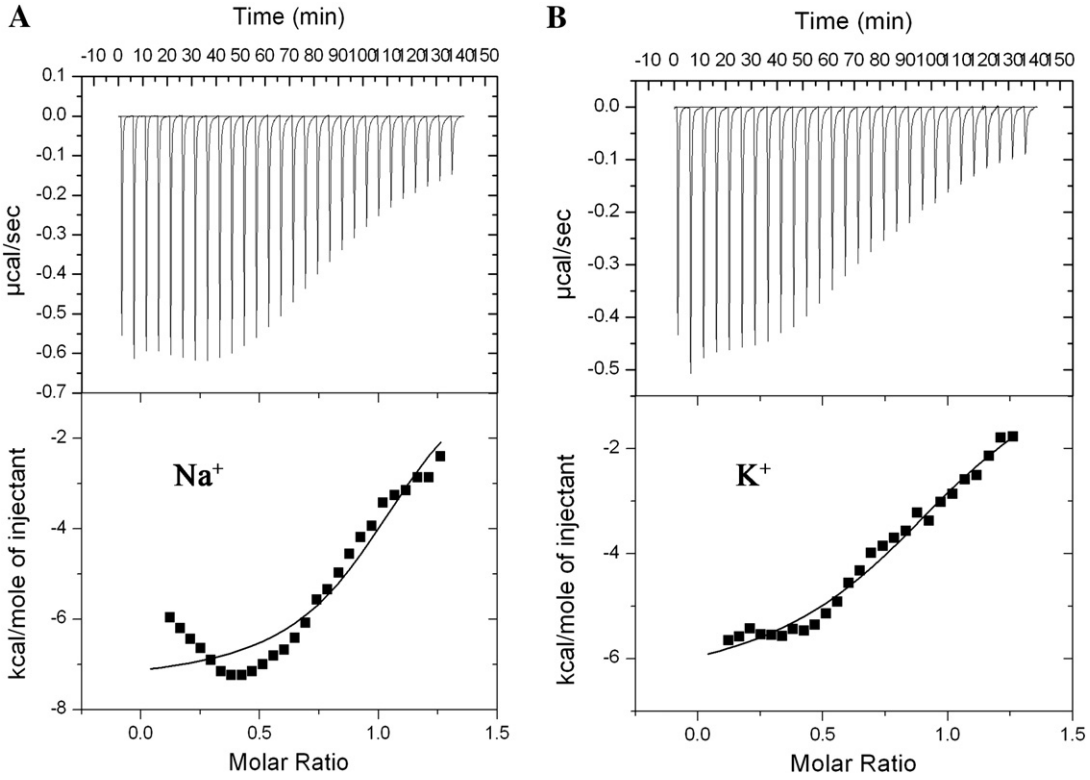

Fig. 4. TMPyP4 could bind to G-quadruplex folded by P-pot1 G18 with different monovalent cations in vitro. A. ITC experiment for titration of 5 μM P-pot1 G18 oligonucleotide with 300 μM TMPyP4 in NaCl-containing buffer. B. ITC experiment for titration of 5 μM P-pot1 G18 oligonucleotide with 100 μM TMPyP4 in KCl-containing buffer.

expression level, as shown in Fig. 7B. We further studied POT1 protein expression levels through Western blot, and it was found that decreasing levels of POT1 protein expression were detected for samples treated with increasing concentration of TMPyP4, as shown in Fig. 7C. In the mean time, we found that the expression level of a transcription factor hnRNP K was not changed upon treatment with up to 10 μM TMPyP4. These results indicated that TMPyP4 could stabilize the G-quadruplex formed by P-pot1 G18 resulting in down-regulations of pot1 mRNA transcription and consequently POT1 protein translation in cancer cells.

3.6. The P-pot1 G18 G-quadruplex formation affected the binding of transcription factor hnRNP K to a nearby C-rich binding site possibly making influence to pot1 transcription

It has been reported that transcription factors play essential roles in gene transcriptional regulation [28], therefore, it is important to know its relationship with DNA secondary structures in regulating gene transcriptions. We analyzed the sequence around P-pot1 G18 and found a binding site for transcription factor protein hnRNP K. hnRNP K belongs to a family of heterogeneous nuclear ribonucleoprotein (hnRNP) complexes associated with RNA polymerase II transcripts in regulating gene transcription process [29]. hnRNP K plays an important role in gene expression processes such as gene transcription, translation, and RNA biosynthesis [30]. hnRNP K closely binds to poly(C) single strand DNA especially in the promoter region, and its minimum binding sequence unit is TCCC [31]. In the present study, we found an hnRNP K protein binding unit TCCC located 8 base pairs away from P-pot1 G18 in the pot1 promoter, and an extended P-pot1 G18 oligonucleotide including this TCCC binding unit was synthesized and named as P-pot1 G18 tccc, as shown in Table 1. In our Ch-IP experiment, we found that hnRNP K could bind to pot1 gene promoter containing P-pot1 G18 tccc sequence in vivo, as shown in Fig. 8A. It should be noted that we used single strand DNA with its major form as G-quadruplex for our in vitro EMSA experiment. In contrast, for our Ch-IP experiment, the double strand DNA was present in cells, with the anti-sense DNA of P-pot1 G18 tccc (TCCCGCCCAGCGGACCCGCCCGCTTCCCCT, named as P-pot1 C18) possibly binding strongly to hnRNP K. It is also possible that G-quadruplex is no longer a predominant form when its anti-sense DNA was present in cells.

Then, we would like to know whether the G-quadruplex formation by P-pot1 G18 could affect this binding process. Therefore, we cloned hnRNP K gene and constructed pET-28(a)–hnRNP K protein expression plasmid. hnRNP K was overexpressed in *Escherichia coli*, and purified to apparent homogeneity as shown in Fig. 8B. The increasing amount of purified protein hnRNP K was then incubated with P-pot1 G18 tccc, and the result was shown in Fig. 8C. We found that our pre-annealed P-pot1 G18 tccc oligonucleotide existed in two forms with a major form of G-quadruplex and a minor form of single strand DNA. With increasing concentration of protein hnRNP K, the single strand DNA

Table 3
Thermodynamic parameters for the binding between P-pot1 G18 and TMPyP4 in reaction buffers containing NaCl or KCl.

	n	Kb (M^{-1})	△H (kcal mol^{-1})	-T△S (kcal mol^{-1})	△G (kcal mol^{-1})
100 mM NaCl	1.08 ± 0.03	$4.62 \times 10^5 \pm 1.50 \times 10^5$	−7395 ± 265	−28	−7367 ± 265
100 mM KCl	1.04 ± 0.02	$1.91 \times 10^5 \pm 0.31 \times 10^5$	−6531 ± 183	−56.5	−6475 ± 183

Fig. 5. Constructed plasmid sequences for luciferase assay.

molecule was gradually diminished while the quantity of intramolecular G-quadruplex was not changed, which indicated that hnRNP K bound with single strand DNA only to form protein–DNA complexes shown on the top of the gel. Two protein–DNA complex bands were observed on the gel, indicating two possible binding modes. This result indicated that G-quadruplex formation repressed the binding of hnRNP K with P-pot1 G18 tccc. Further CD experiment was carried out, and the result was shown in Fig. 8D. P-pot1 G18 tccc gave a CD spectrum with a valley at 245 nm and two peaks at 260 nm and 285 nm in buffer containing KCl, indicating a mixed-type G-quadruplex structure. After addition of protein hnRNP K, the CD signal peaks and their intensities were not changed, which also indicated no binding between protein hnRNP K and the G-quadruplex structure. The above results showed that the G-quadruplex formation by P-pot1 G18 affected the binding of transcription factor hnRNP K to a nearby C-rich binding site possibly adding influence to pot1 transcription.

3.7. Transcription factor hnRNP K could up-regulate the translation of POT1 protein in vivo

In order to further study the role of hnRNP K on pot1 transcription and translation, we constructed pEGFP–hnRNP K plasmid, a eukaryotic fusion expression system, which could express hnRNP K and green fluorescent fusion protein. Through laser scanning confocal

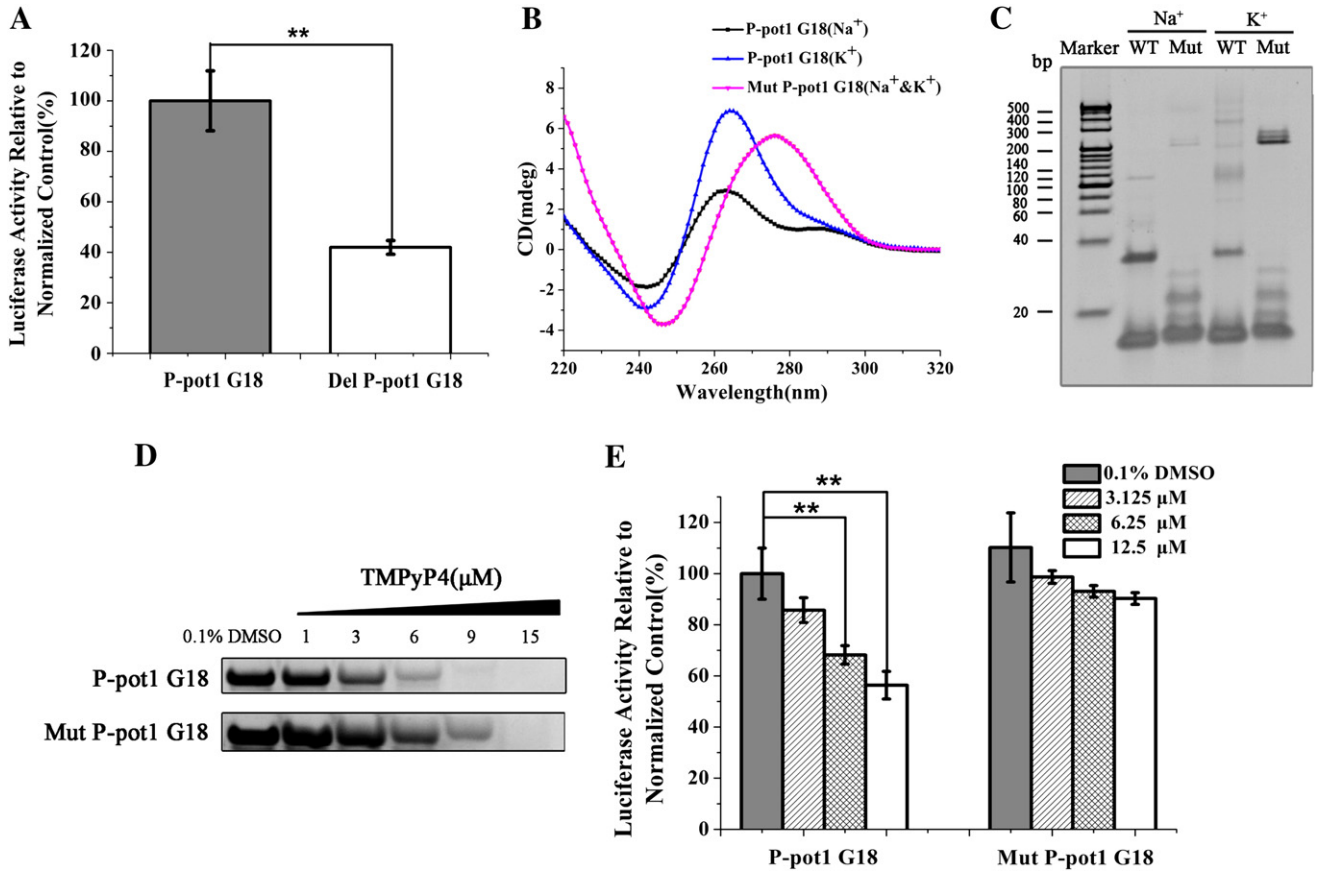

Fig. 6. G-quadruplex folded by P-pot1 G18 down-regulated pot1 gene transcription. A. Luciferase assay for P-pot1 G18 wild type plasmid in comparison with the plasmid without P-pot1 G18. The symbol ** indicates a significant difference at $P < 0.01$ vs wild type. B. Circular dichroism experiments for Mut P-pot1 G18 oligonucleotide compared to P-pot1 G18 oligonucleotide in NaCl and KCl-containing buffers. The pink line is circular dichroism spectrum of Mut P-pot1 G18 oligonucleotide in NaCl and KCl-containing buffers. C. EMSA assay result for Mut P-pot1 G18 oligonucleotide compared to P-pot1 G18 oligonucleotide in NaCl and KCl-containing buffers. Lane WT is for P-pot1 G18, while lane Mut is for Mut P-pot1 G18. D. PCR stop assay for Mut P-pot1 G18 oligonucleotide compared to P-pot1 G18 oligonucleotide. TMPyP4 was used in this experiment. E. Luciferase assay for P-pot1 G18 wild type plasmid in comparison with Mut P-pot1 G18 plasmid. After Hela cells were transfected with these plasmids in the logarithmic phase, different concentrations of TMPyP4 were added to the Hela cells followed with incubation for 48 h. The symbol ** indicates a significant difference at $P < 0.01$ vs 0.1% DMSO, respectively.

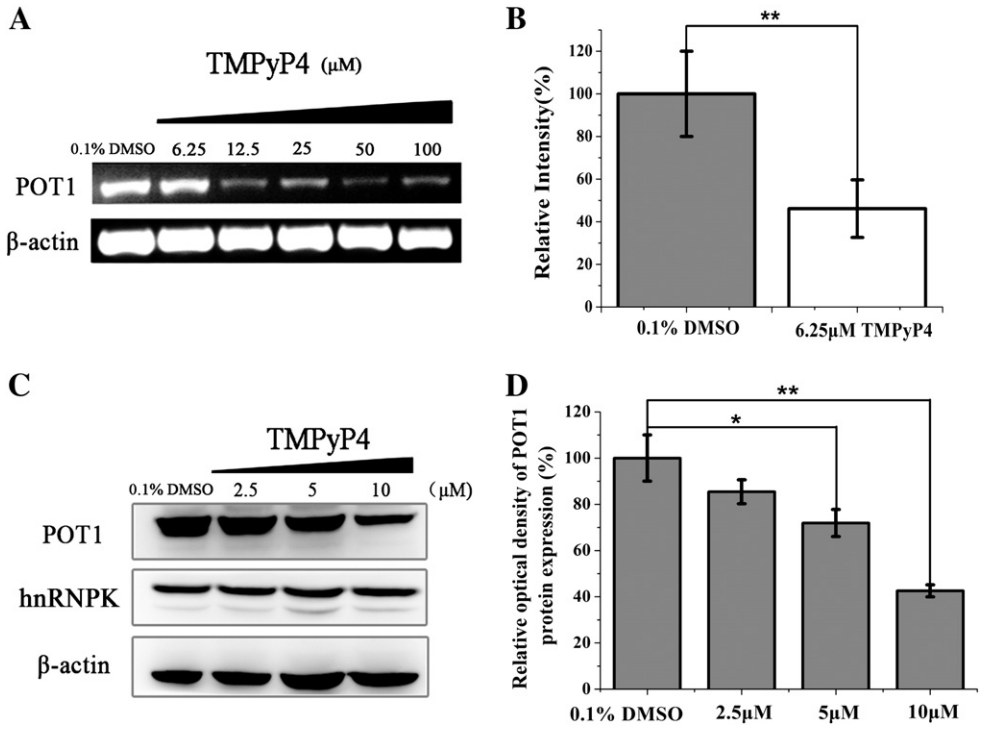

Fig. 7. Formation of G-quadruplex by P-pot1 G18 down-regulated expression of POT1 protein. A. RT-PCR experiment for Hela cells treated with 0.1% DMSO and TMPyP4 ranged from 0 to 100 μM for 48 h. B. qRT-PCR experiment for Hela cells treated with 6.25 μM TMPyP4 for 48 h, and the symbol ** indicates a significant difference at $P < 0.01$ vs 0.1% DMSO. C. Western blot for Hela cells treated with 0.1% DMSO and 2.5, 5 and 10 μM TMPyP4 for 48 h. D. Optical density analysis of (C) for POT1 expression. The symbol * indicates a significant difference at $P < 0.05$ vs 0.1% DMSO, and the symbol ** indicates a significant difference at $P < 0.01$ vs 0.1% DMSO.

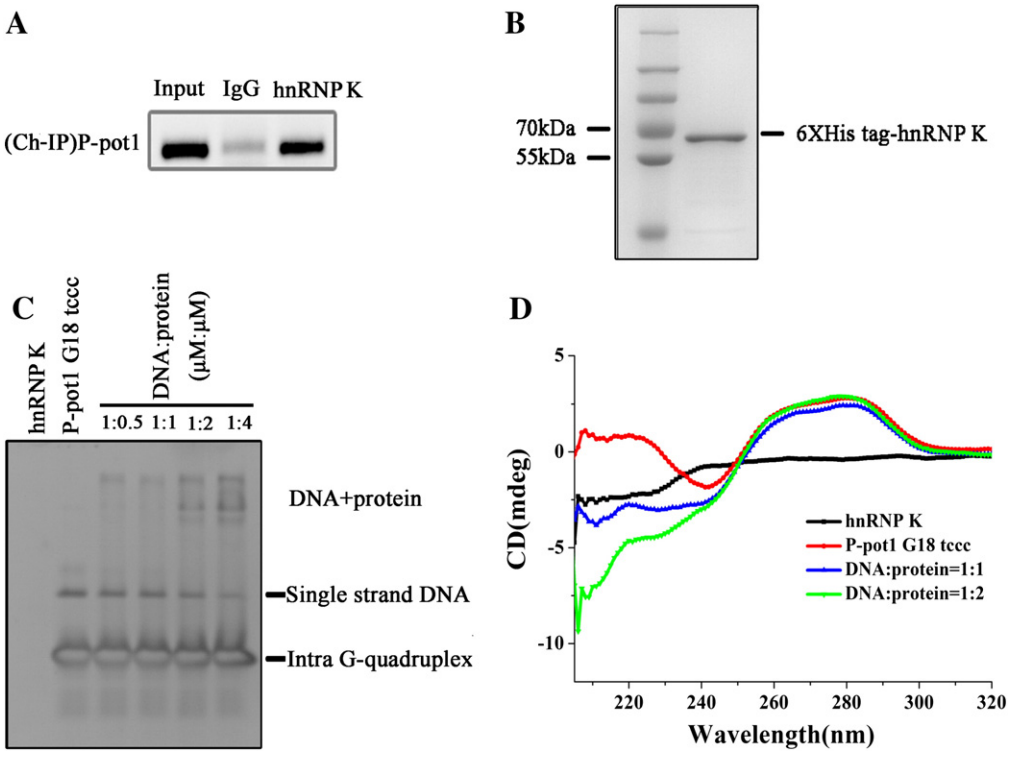

Fig. 8. Formation of G-quadruplex by P-pot1 G18 caused reduced binding affinity for transcription factor in proximal position. A. Ch-IP experiment for the binding of hnRNP K with pot1 promoter region. IgG sample was negative control. B. SDS-PAGE for purified hnRNP K protein. C. EMSA experiment for the binding of hnRNP K with P-pot1 G18 tccc. The reaction buffer contained 10 mM Tris–HCl (pH 7.5) and 100 mM KCl. DNA samples were denatured at 95 °C for 5 min, subsequently cooled to room temperature, and then incubated with hnRNP K for 1 h at 37 °C at different ratios. The DNA final concentration was 10 μM. D. Circular dichroism spectrum for the binding of hnRNP K protein with P-pot1 G18 tccc sequence. The reaction volume for CD was 700 μL, and the DNA concentration was 2 μM. The data were plotted by using the DNA to protein ratios of 1:1 and 1:2 after deduction of buffer.

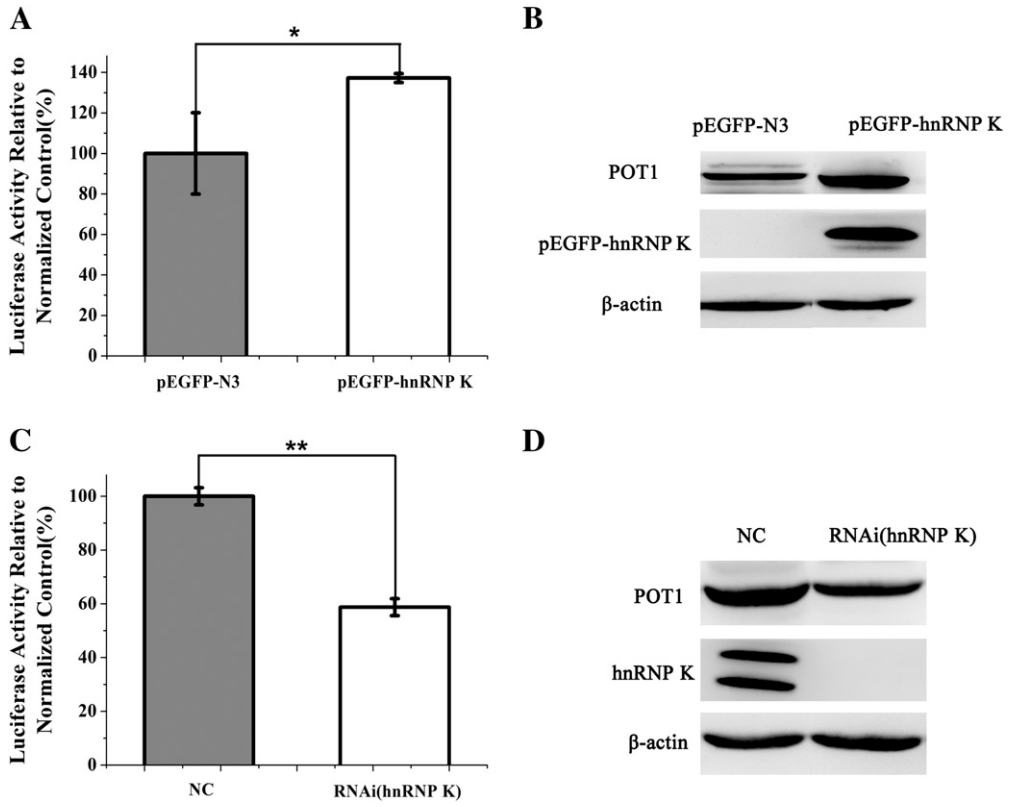

Fig. 9. hnRNP K protein up-regulated the expression of POT 1 protein. A. Luciferase assay after co-transfection of hnRNP K over-expression plasmid (pEGFP–hnRNP K) and recombinant luciferase reporter plasmid (P-pot1 G18) into Hela cells followed with a 36 h cell incubation, and symbol * indicates a significant difference at $P < 0.05$ vs pEGFP-N3 vector. B. Western blot after transfection of hnRNP K over-expression plasmid (pEGFP–hnRNP K) into Hela cells followed with a 36 h cell incubation. C. Luciferase assay after RNA interference of hnRNP K protein expression and co-transfection of recombinant luciferase reporter plasmid (P-pot1 G18) into Hela cells followed with a 36 h cell incubation, and symbol ** indicates a significant difference at $P < 0.01$ vs NC sample. D. Western blot for RNA interference of hnRNP K protein expression in Hela cells followed with a 36 h cell incubation.

microscopy technology, we found green fluorescent protein expressed by pEGFP–hnRNP K plasmid in Hela cells 36 h after transfection (Supporting Information Figure S2). As shown in Fig. 9A and B, significantly increased POT1 protein level was observed when hnRNP K protein over-expressed 36 h in Hela cells. We also studied the influence of hnRNP K protein on pot1 transcription and translation through interfering hnRNP K expression, and the siRNA-hnRNP K primers are shown in Table 1. As shown in Fig. 9C and D, significantly decreased POT1 level was observed after hnRNP K was interfered followed with the incubation of the Hela cells for 36 h for protein expression. These results showed that transcription factor hnRNP K could have a strong influence on the transcription and translation of pot1 gene in cellulo. Our results also showed that interfering hnRNP K protein expression and G-quadruplex formation by P-pot1 G18 had the same influence both down-regulating pot1 gene expression in cellulo. Our results might indicate that the G-quadruplex formation affected the binding of transcription factor hnRNP K to a nearby region in pot1 gene promoter consequently making additional influence for down-regulation of pot1 gene transcription.

4. Discussion and conclusion

The GC-rich regions, possibly forming quadruplex in living cells, play an important role in human genome [32]. Recently, G-quadruplex structures have been detected in human genomic DNA with hf2 antibody [18]. G-quadruplexes have been studied from physical, chemical, and biological points of view because of their unique structure and stability under physiological conditions [33]. Over the years, more and more researches about promoter G-quadruplex have been published, such as c-*MYC*, Bcl-2, KRAS, and VEGF [34]. POT1 is a telomere binding protein in a telomere binding complex Shelterin, and is required for both chromosomal end protection and telomere length regulation. It has been reported that deficiency of POT1 would initiate DNA damage checkpoint activation and aberrant homologous recombination at telomeres [35]. Human POT1 is unable to lengthen the telomeres of telomerase-negative cells unless telomerase activity is induced, which indicates that a normal function of POT1 is to facilitate telomere elongation by telomerase [36]. The full length human POT1 has a molecular weight of 70 kDa, but recently at least three consistently occurring forms with molecular weight of 90, 70 and 45 kDa have been reported because of post-translational modifications, which also affect its intracellular localization and function [37]. However, transcriptional regulation of POT1 expression, especially the role of its promoter sequence, has not been studied. In the present research, we found a parallel G-quadruplex formed by a 30-base sequence (named P-pot1 G18) located from −165 to −136 base pairs upstream of the translation starting site of pot1 gene. Since TMPyP4 has been widely used in research of promoter G-quadruplex [38], here we used this compound as a probe to study the role of G-quadruplex in the promoter of pot1 gene.

Our CD results showed that P-pot1 G18 could fold into parallel G-quadruplex in buffer containing 100 mM KCl, and the amount of G-quadruplex increased with increasing concentration of KCl. In comparison, in buffer containing NaCl, P-pot1 G18 could fold into a mixed type G-quadruplex composed of mainly parallel G-quadruplex, and the amount of G-quadruplex was not changed with increasing concentration of NaCl. Our EMSA result showed that at least three types of P-pot1 G18 structures could exist, including intra-molecular G-quadruplex, single-strand DNA, and inter-molecular G-quadruplex. Because P-pot1 G18 has five guanine-rich sections, it may have several types of G-quadruplex topologies. Our mutation experiment of P-pot1 G18 indicated that its first three guanine-rich sections play more

important roles for the formation of G-quadruplex, since Mut1, Mut2 and Mut3 behaved quite differently from the wild-type in CD and EMSA. Our CD melting experiment showed that TMPyP4 could stabilize the G-quadruplex formed by P-pot1 G18 in buffer containing either NaCl or KCl, but its stability is a little different. The G-quadruplex is more stable in buffer containing KCl, and its stability was also more enhanced by TMPyP4. Our ITC experiment showed that TMPyP4 and the G-quadruplex formed an interaction complex with a stoichiometry of 1:1, and this process was exothermic and enthalpy driven. TMPyP4 could bind to the G-quadruplex in buffer containing either NaCl or KCl, and their binding affinity in NaCl-containing buffer was higher than that in KCl-containing buffer. The above results showed that although TMPyP4 could bind to the G-quadruplex more strongly in NaCl-containing buffer rather than in KCl-containing buffer at low temperature, the thermostability of the binding complex in KCl-containing buffer is higher rather than in NaCl-containing buffer, which may be explained by their different binding mode properties with different monovalent cations, similar to that reported previously [25].

After above characterization of the G-quadruplex in vitro, we studied its biological significance in regulation of gene transcription. Our deletion experiment indicated that P-pot1 G18 could play an important role in pot1 gene transcription. Our mutation experiment with recombinant plasmid followed by treatment with TMPyP4 showed that the G-quadruplex formation could repress pot1 gene transcription, as measured with the luciferase activity. Our PCR stop assay showed that the G-quadruplex formation could down-regulate both pot1 gene transcription and protein expression in cancer cells. It has been reported that transcription factors play an important role in the transcription process [39], therefore, we studied whether the G-quadruplex formation could affect the binding of transcription factor. A binding site for transcription factor hnRNP K was found close to the G-quadruplex, which was investigated in the present study. hnRNP K is a well-known transcription factor which specifically binds to TCCC sequence [40]. The expression level of hnRNP K was not affected by up to 10 μM TMPyP4 in cancer cells. Our Ch-IP experiment showed that hnRNP K could bind to pot1 gene promoter region including P-pot1 G18 tccc sequence in vivo. Our EMSA and CD experimental results indicated that P-pot1 G18 tccc could fold into intra-molecular G-quadruplex as a major form with single-strand DNA as a minor form in vitro, and hnRNP K could bind to the single-strand P-pot1 G18 tccc only. Our co-transfection luciferase assay and Western blot result showed that when hnRNP K protein over-expressed in Hela cells, POT1 protein expression level was significantly increased. On the contrary, POT1 protein expression level was significantly decreased when hnRNP K protein expression was interfered. The interference of hnRNP K protein expression and G-quadruplex formation by P-pot1 G18 on pot1 gene promoter had the same effect both down-regulating pot1 gene expression in cellulo. These results indicated that the formation of G-quadruplex by P-pot1 G18 could prevent hnRNP K from binding to the promoter region, consequently making an additional effect in down-regulating pot1 gene transcription.

In summary, our extensive experimental studies indicated that P-pot1 G18 G-quadruplex might become a potentially new drug target for antitumor agents. Our results indicated that transcription factor hnRNP K could up-regulate pot1 gene transcription upon its binding with pot1 promoter. P-pot1 G18 G-quadruplex formation could affect the binding of transcription factor hnRNP K to its nearby region, and thus making additional influence to gene transcription.

Acknowledgement

We thank the National Natural Science Foundation of China (Grants 21242010, 91213302, 21172272, and 81330077) and Sun Yat-sen University for financial support of this study.

Appendix A. Supplementary data

Supplementary data to this article can be found online at http://dx.doi.org/10.1016/j.bbagen.2014.03.001.

References

[1] E.H. Blackburn, Structure and function of telomeres, Nature 350 (1991) 569–573.
[2] R.J. Hodes, Telomere length, aging, and somatic cell turnover, J. Exp. Med. 190 (1999) 153–156.
[3] B. McClintock, The stability of broken ends of chromosomes in *Zea mays*, Genetics 26 (1941) 234–282.
[4] D. Gilley, H. Tanaka, B.S. Herbert, Telomere dysfunction in aging and cancer, Int. J. Biochem. Cell Biol. 37 (2005) 1000–1013.
[5] R.K. Moyzis, J.M. Buckingham, L.S. Cram, M. Dani, L.L. Deaven, M.D. Jones, J. Meyne, R. L. Ratliff, J.R. Wu, A highly conserved repetitive DNA sequence, (TTAGGG)n, present at the telomeres of human chromosomes, Proc. Natl. Acad. Sci. U. S. A. 85 (1988) 6622–6626.
[6] K. Masutomi, E.Y. Yu, S. Khurts, I. Ben-Porath, J.L. Currier, G.B. Metz, M.W. Brooks, S. Kaneko, S. Murakami, J.A. DeCaprio, R.A. Weinberg, S.A. Stewart, W.C. Hahn, Telomerase maintains telomere structure in normal human cells, Cell 114 (2003) 241–253.
[7] P. Boukamp, S. Popp, D. Krunic, Telomere-dependent chromosomal instability, J. Investig. Dermatol. Symp. Proc. 10 (2005) 89–94.
[8] M.A. Blasco, Telomere length, stem cells and aging, Nat. Chem. Biol. 3 (2007) 640–649.
[9] T. de Lange, Shelterin: the protein complex that shapes and safeguards human telomeres, Genes Dev. 19 (2005) 2100–2110.
[10] B. van Steensel, T. de Lange, Control of telomere length by the human telomeric protein TRF1, Nature 385 (1997) 740–743.
[11] A. Smogorzewska, B. van Steensel, A. Bianchi, S. Oelmann, M.R. Schaefer, G. Schnapp, T. de Lange, Control of human telomere length by TRF1 and TRF2, Mol. Cell. Biol. 20 (2000) 1659–1668.
[12] F. Wang, E.R. Podell, A.J. Zaug, Y. Yang, P. Baciu, T.R. Cech, M. Lei, The POT1–TPP1 telomere complex is a telomerase processivity factor, Nature 445 (2007) 506–510.
[13] M. Lei, E.R. Podell, T.R. Cech, Structure of human POT1 bound to telomeric single-stranded DNA provides a model for chromosome end-protection, Nat. Struct. Mol. Biol. 11 (2004) 1223–1229.
[14] H. Hwang, N. Buncher, P.L. Opresko, S. Myong, POT1–TPP1 regulates telomeric overhang structural dynamics, Structure 20 (2012) 1872–1880.
[15] T. de Lange, How telomeres solve the end-protection problem, Science 326 (2009) 948–952.
[16] A.J. Ramsay, V. Quesada, M. Foronda, L. Conde, A. Martinez-Trillos, N. Villamor, D. Rodriguez, A. Kwarciak, C. Garabaya, M. Gallardo, M. Lopez-Guerra, A. Lopez-Guillermo, X.S. Puente, M.A. Blasco, E. Campo, C. Lopez-Otin, POT1 mutations cause telomere dysfunction in chronic lymphocytic leukemia, Nat. Genet. 45 (2013) 526–530.
[17] J.L. Huppert, S. Balasubramanian, Prevalence of quadruplexes in the human genome, Nucleic Acids Res. 33 (2005) 2908–2916.
[18] E.Y. Lam, D. Beraldi, D. Tannahill, S. Balasubramanian, G-quadruplex structures are stable and detectable in human genomic DNA, Nat. Commun. 4 (2013) 1796.
[19] S. Balasubramanian, S. Neidle, G-quadruplex nucleic acids as therapeutic targets, Curr. Opin. Chem. Biol. 13 (2009) 345–353.
[20] A. Siddiqui-Jain, C.L. Grand, D.J. Bearss, L.H. Hurley, Direct evidence for a G-quadruplex in a promoter region and its targeting with a small molecule to repress c-MYC transcription, Proc. Natl. Acad. Sci. U. S. A. 99 (2002) 11593–11598.
[21] C.L. Grand, H. Han, R.M. Munoz, S. Weitman, D.D. Von Hoff, L.H. Hurley, D.J. Bearss, The cationic porphyrin TMPyP4 down-regulates c-MYC and human telomerase reverse transcriptase expression and inhibits tumor growth in vivo, Mol. Cancer Ther. 1 (2002) 565–573.
[22] M. Corriveau, M.R. Mullins, D. Baus, M.E. Harris, D.J. Taylor, Coordinated interactions of multiple POT1–TPP1 proteins with telomere DNA, J. Biol. Chem. 288 (2013) 16361–16370.
[23] J. Seenisamy, E.M. Rezler, T.J. Powell, D. Tye, V. Gokhale, C.S. Joshi, A. Siddiqui-Jain, L.H. Hurley, The dynamic character of the G-quadruplex element in the c-MYC promoter and modification by TMPyP4, J. Am. Chem. Soc. 126 (2004) 8702–8709.
[24] M. Inoue, D. Miyoshi, N. Sugimoto, Structural switch of telomere DNA by pH and monovalent cation, Nucleic Acids Symp. Ser. (Oxf) (2005) 243–244.
[25] D.F. Shi, R.T. Wheelhouse, D. Sun, L.H. Hurley, Quadruplex-interactive agents as telomerase inhibitors: synthesis of porphyrins and structure–activity relationship for the inhibition of telomerase, J. Med. Chem. 44 (2001) 4509–4523.
[26] E.J. Andrew, S. Merchan, C. Lawless, A.P. Banks, D.J. Wilkinson, D. Lydall, Pentose phosphate pathway function affects tolerance to the G-quadruplex binder TMPyP4, PLoS One 8 (2013) e66242.
[27] D. Peng, J.H. Tan, S.B. Chen, T.M. Ou, L.Q. Gu, Z.S. Huang, Bisaryldiketene derivatives: a new class of selective ligands for c-myc G-quadruplex DNA, Bioorg. Med. Chem. 18 (2010) 8235–8242.
[28] M.K. Ray, C.Y. Chen, R.J. Schwartz, F.J. DeMayo, Transcriptional regulation of a mouse Clara cell-specific protein (mCC10) gene by the NKx transcription factor family members thyroid transcription factor 1 and cardiac muscle-specific homeobox protein (CSX), Mol. Cell. Biol. 16 (1996) 2056–2064.

[29] M.J. Matunis, W.M. Michael, G. Dreyfuss, Characterization and primary structure of the poly(C)-binding heterogeneous nuclear ribonucleoprotein complex K protein, Mol. Cell. Biol. 12 (1992) 164–171.
[30] K.W. Hsueh, S.L. Fu, C.Y. Huang, C.H. Lin, Aurora-A phosphorylates hnRNPK and disrupts its interaction with p53, FEBS Lett. 585 (2011) 2671–2675.
[31] E.F. Michelotti, G.A. Michelotti, A.I. Aronsohn, D. Levens, Heterogeneous nuclear ribonucleoprotein K is a transcription factor, Mol. Cell. Biol. 16 (1996) 2350–2360.
[32] N. Maizels, L.T. Gray, The G4 genome, PLoS Genet. 9 (2013) e1003468.
[33] T. Endoh, Y. Kawasaki, N. Sugimoto, Suppression of gene expression by G-quadruplexes in open reading frames depends on G-quadruplex stability, Angew. Chem. Int. Ed. Engl. 52 (2013) 5522–5526.
[34] S. Cogoi, L.E. Xodo, G-quadruplex formation within the promoter of the KRAS proto-oncogene and its effect on transcription, Nucleic Acids Res. 34 (2006) 2536–2549.
[35] L. Wu, A.S. Multani, H. He, W. Cosme-Blanco, Y. Deng, J.M. Deng, O. Bachilo, S. Pathak, H. Tahara, S.M. Bailey, R.R. Behringer, S. Chang, Pot1 deficiency initiates DNA damage checkpoint activation and aberrant homologous recombination at telomeres, Cell 126 (2006) 49–62.
[36] L.M. Colgin, K. Baran, P. Baumann, T.R. Cech, R.R. Reddel, Human POT1 facilitates telomere elongation by telomerase, Curr. Biol. 13 (2003) 942–946.
[37] U. Singh, V. Maturi, B. Westermark, Evidence for multiple forms and modifications of human POT1, DNA Repair (Amst) 8 (2013) 876–887.
[38] V.H. Le, N. Nagesh, E.A. Lewis, Bcl-2 promoter sequence G-quadruplex interactions with three planar and non-planar cationic porphyrins: TMPyP4, TMPyP3, and TMPyP2, PLoS One 8 (2013) e72462.
[39] W.J. Yang, M.J. Song, E.Y. Park, J.J. Lee, J.H. Park, K. Park, H.P. Kim, Transcription factors Sp1 and Sp3 regulate expression of human ABCG2 gene and chemoresistance phenotype, Mol. Cells 36 (2013) 368–375.
[40] J.P. Stains, F. Lecanda, D.A. Towler, R. Civitelli, Heterogeneous nuclear ribonucleoprotein K represses transcription from a cytosine/thymidine-rich element in the osteocalcin promoter, Biochem. J. 385 (2005) 613–623